Nature and kinetics of extracellular peptidases in subsurface sediments of the White Oak River estuary, NC

Andrew D. Steen[1,*], Richard T. Kevorkian[2], Jordan T. Bird[2], Nina Dombrowski[3], Brett J. Baker[3], Shane M. Hagen[1], Katherine H. Mulligan[1,4], Jenna M. Schmidt[1], Austen T. Webber[1], Marc J. Alperin[5]

[1]Department of Earth and Planetary Sciences, University of Tennessee, Knoxville, Tennessee, USA

[2]Department of Microbiology, University of Tennessee, Knoxville, Tennessee, USA

[3]Department of Marine Science, University of Texas-Austin, Marine Science Institute, Port Aransas, Texas, USA

[4]Department of Biology, University of North Carolina at Chapel Hill, Knoxville, Tennessee, USA

[5]Department of Marine Sciences, University of North Carolina at Chapel Hill, USA

[*]Corresponding: email: asteen1@utk.edu

mail: 306 EPS Building, 1412 Circle Drive, Knoxville, TN 37996-1410

tel: (865) 974-4014, fax: 865 974 2638

Abstract

Microbial communities inhabiting subsurface sediments contain abundant heterotrophs, which oxidize organic matter to obtain carbon and energy. Subsurface sediments contain very low concentrations of bioavailable compounds, and it is not clear what fraction of sedimentary organic matter heterotrophs are able to access. To gain a more mechanistic understanding of heterotrophy in subsurface sediments of the White Oak River, NC, we examined the genetic potential for extracellular peptidase production encoded within metagenome-assembled genomes, and experimentally assayed the kinetics of a wide range of extracellular peptidases in bulk sediments. We identified genes coding for at least 15 classes of extracellular peptidases and observed enzyme-catalyzed hydrolysis of 11 different peptidase substrates. Potential activities (V_{max}) of extracellular peptidases decreased downcore, but cell-specific V_{max} was relatively constant and similar to values observed in seawater phytoplankton blooms. Half-saturation constants also decreased downcore, and the relative contribution of enzymes relevant to degraded organic matter increased with increasing depth. Together, these results suggest a subsurface community that accesses organic matter using mechanisms that are basically similar to those in surface environments, but which is adapted to the highly degraded organic matter that is present in the subsurface.

Introduction

Marine sediments are one of the largest microbial environments on earth (Kallmeyer *et al.*, 2012). Many sedimentary microbes appear to be heterotrophs, slowly metabolizing organic matter (Jørgensen and Marshall, 2016; Biddle *et al.*, 2006), but the mechanisms by which these heterotrophs access old, unreactive organic carbon remain poorly characterized.

In surface environments, where photosynthesis fuels carbon fixation, heterotrophic microorganisms gain energy from a combination of small molecules (<600-1000 Da), which can be taken up directly via general uptake porins (Benz and Bauer, 1988) and macromolecules, which must be broken down outside of the cell by extracellular enzymes. Because most freshly-produced organic matter is macromolecular and large molecules tend to be more bioavailable than small ones (Benner and Amon, 2015), the nature and activity of extracellular enzymes present in surface environments is a major control on the rate of microbial carbon oxidation in such environments.

It is not clear whether microbial extracellular enzymes play the same role in subsurface sediments. Extracellular peptidase activity has been identified in sapropels up to 389 cm below seafloor (cmbsf) in the eastern Mediterranean Sea (Coolen and Overmann, 2000; Coolen *et al.*, 2002), in sediment from 600-630 cmbsf in Aarhus Bay sediments (Lloyd *et al.*, 2013b) and in the interior of seafloor basalts at the Loihi seamount (Jacobson Meyers *et al.*, 2014). However, the nature and relative importance of extracellular enzymes in subsurface environments remains poorly constrained because these studies examined few samples, and only limited enzymatic classes and sample numbers were assayed. It is possible that, like heterotrophs in surface environments,

65 heterotrophs in subsurface environments mainly gain access to organic carbon via
66 extracellular enzymes. On the other hand, some of the unique aspects of subsurface
67 sediments suggest that extracellular enzymes might not be an effective strategy to obtain
68 carbon or energy. First, subsurface sediments contain markedly fewer bioavailable
69 compounds such as amino acids and sugars than do surface sediments (Burdige, 2007).
70 Therefore, these compounds may be insufficiently abundant to be viable heterotrophic
71 substrates. Second, in order for the production of extracellular enzymes to be part of a
72 viable metabolic strategy, each enzyme must, over its lifetime, provide the cell with at
73 least as much carbon or energy as was required to synthesize the enzyme (Vetter *et al.*,
74 1998; Allison, 2005; Schimel and Weintraub, 2003). In subsurface sediments, where
75 metabolic rates may be orders of magnitude slower at the surface, enzyme lifetimes
76 would need to be correspondingly longer to become 'profitable'. Since enzyme lifetimes
77 are finite, there must exist a community metabolic rate below which extracellular enzyme
78 lifetimes are too short to become profitable. Unfortunately that limit is difficult to
79 quantify because enzyme lifetimes in any environment are poorly constrained (e.g., Steen
80 and Arnosti, 2011).

81 It is also possible that extracellular enzymes are not the primary mechanism by
82 which heterotrophs access sedimentary organic matter. More exotic mechanisms, such as
83 abiotic liberation by reactive species formed from radioactive decay of naturally-present
84 radioisotopes (e.g. Blair *et al.*, 2007) are conceivable, but have not been demonstrated.
85 The goals of this work are to determine whether subsurface heterotrophic communities
86 make substantial use of extracellular enzymes to access organic matter, and if so, to
87 characterize the set of enzymes used.

We investigated genes for extracellular enzymes and the activities of corresponding enzymes in sediments of the White Oak River, NC by estimating the presence of peptidase families in available metagenomic sequencing data and complementing this by measuring the hydrolysis rates of eleven potential peptidase substrates. This site was chosen because the porewater geochemistry and microbiology of these sediments has been well-characterized (Martens and Goldhaber, 1978; Kelley *et al.*, 1990; Baker *et al.*, 2015; Lazar *et al.*, 2016; Lloyd *et al.*, 2011) and because they contain abundant Bathyarchaeota and Marine Benthic Group D archaea, which appear to be capable of metabolizing detrital organic matter (Kubo *et al.*, 2012; Lloyd *et al.*, 2013b; Meng *et al.*, 2014). We focused on peptidases because protein degradation appears to be an important metabolism for some subsurface archaea (Lloyd *et al.*, 2013b) and because peptidases were more active than other enzymes in similar environments (Coolen and Overmann, 2000; Jacobson Meyers *et al.*, 2014). Because environmental samples contain a wide range of distinct peptidases at variable activities (Obayashi and Suzuki, 2005; Steen and Arnosti, 2013) we measured the hydrolysis of eleven different substrates that may be hydrolyzed by structurally and genetically diverse extracellular peptidases. By measuring potential activities (i.e., the capacity of the enzyme to catalyze hydrolysis if substrate concentrations were not limiting) and substrate affinities of microbial extracellular enzymes, we illuminated some of the mechanisms by which subsurface heterotrophic communities access organic carbon.

Materials and Methods

STUDY SITE

Samples were collected from Station H in the White Oak River Estuary, 34° 44.490' N, 77° 07.44' W, first described by Gruebel and Martens (1984). The White Oak River Estuary occupies a drowned river valley in the coastal plain of North Carolina. Station H is characterized by salinity in the range of 10 to 28 and water depth on the order of 2 m. The flux of ΣCO_2 across the sediment-water interface was 0.46 ± 0.02 mmol m^{-2} hr^{-1} (measured in May of 1987), primarily due to organic carbon oxidation via sulfate reduction, and the sediment accumulation rate averages 0.3 cm yr^{-1} (Kelley *et al.*, 1990). Total organic carbon content is approximately 5%. For this study, push cores of 40-85 cm were collected from Station H by swimmers on May 28, 2013, June 14, 2014, and October 22, 2014. In 2013, cores were transported to the nearby Institute of Marine Sciences (University of North Carolina) at Morehead City, where they were sectioned and processed for enzyme activities, porewater geochemistry, and cell counts within 6 hours of sample collection. Porewater sulfate in 2013 was depleted by 43.5 cm, and methane peaked at 79.5 cm (Fig. S1). In 2014, cores were transported on the day of sampling to the University of Tennessee, Knoxville, stored at 4 °C, and processed for enzyme activities the following day. Samples for metagenomic analysis were collected separately in October 2010 from three sites (sites 1, 2, and 3, as previously described by Baker et al (2015)), all of which are within 550 m of Station H.

METAGENOMIC ANALYSIS

To resolve the taxonomic distribution of extracellular peptidases we searched a pre-existing White Oak River *de novo* assembled and binned metagenomic dataset (Table S2; Baker *et al.*, 2015) for genes that were assigned extracellular peptidase functions. These assignments were based on best matches to extracellular peptidases in KEGG, pfam, and NCBI-nr (non-redundant) databases using the IMG annotation pipeline (Markowitz et al., 2014). Genes were additionally screened for signal peptidase motifs using the following programs: PrediSI setting the organism group to gram-negative bacteria (Hiller *et al.*, 2004), PRED-Signal trained on archaea (Bagos *et al.*, 2009), the standalone version of PSORT v.3.0 trained against archaea (Yu *et al.*, 2010), and SignalIP 4.1 using gram-negative bacteria as the organism group (Petersen *et al.*, 2011). All programs were used with default settings if not stated otherwise. Results are provided in Supplementary Table 1.

In total, binned genomes from three different depth zones of White Oak River sediments were examined. The sulfate-rich zone (SRZ) genomes were obtained from sites 2 and 3 core sections 8-12 and 8-10 cm, respectively. The sulfate-methane transitions zone (SMTZ) genomes were recovered from site 2 and 3 and depths of 30-32 cm and 24-28 cm. The methane-rich zone (MRZ) was from site 1 and 52-54 cm. Many of these genes were binned to Bacteria (Baker et al. 2015) and Archaea community members (Baker *et al.*, 2016; Lazar *et al.*, 2016; Seitz *et al.*, 2016). Taxonomic assignments of peptidases identified in the community were based on this binning information. However, since not all of the peptidases were binned, we used top matches to NCBI to identify the unbinned genes. The majority of the Archaea present in the shallow (8-12 cm) sulfate-

rich zone were confidently binned, thus were used to determine the relative contributions of archaeal extracellular peptidases (Fig 1b). A smaller proportion (68% of SRZ, 24% of SMTZ, and 27% of MRZ) of the bacterial peptidase genes were confidently binned, therefore, classification was based on top BLAST hits to NCBI. These classifications were then refined using the bin assignments.

ENZYME ASSAYS

Enzyme assays were performed using different protocols in 2013 versus 2014. In 2013, enzyme assays were performed according to a protocol similar to the one described in Lloyd et al (2013b). Cores were sectioned into 3 cm intervals. The following intervals were selected for enzyme assays: 0-3 cm, 3-6 cm, 27-30 cm, 57-60 cm, and 81-83 cm. Each section was homogenized, and approximately 0.5 ml wet sediment was transferred into separate 5 ml amber glass serum vials, which had been pre-weighed and preloaded with 4 ml anoxic artificial seawater (Sigma Sea Salts, salinity = 15, pH=7.5) Samples were weighed again to determine the precise mass of wet sediment added, and then an appropriate quantity of 20 mM peptidase substrate stock dissolved in DMSO was added, up to 90 μL, for final substrate concentrations of 0, 25, 50, 75, 100, 200, or 300 μM. Triplicate incubations with 400 μM Arg-AMC, Gly-AMC, Leu-AMC and Gly-Gly-Arg-AMC were also created, but these were omitted for Ala-Ala-Phe-AMC and Boc-Phe-Val-Arg-AMC because the latter two substrates are considerably more expensive. Each serum vial was vortexed, briefly gassed with N_2 to remove oxygen introduced with the sample, and approximately 1.3 ml slurry was immediately removed, transferred to a microcentrifuge tube, and placed on ice to quench the reaction. The precise time of quenching was recorded. This was centrifuged at 10,000 × *g* within approximately 15

minutes. The supernatant was transferred to a methacrylate cuvette and fluorescence was measured with a Turner Biosystems TBS-380 fluorescence detector set to "UV" (λ_{ex}=365-395 nm, λ_{em}=465-485 nm). Samples were then incubated at 16 °C, approximately the in situ temperature, and the sampling procedure was repeated after approximately 3 hours. The rate of fluorescence production was calculated as the increase in fluorescence for each sample divided by the elapsed time between sample quenching. Killed controls were made using homogenized, autoclaved sediments from 35-45 cmbsf. However, we note that autoclaving does not destroy sediment enzymes because sorption to mineral surfaces stabilizes enzyme structure, vastly increasing their ability to maintain a functional conformation at high temperatures (Stursova and Sinsabaugh, 2008; Carter *et al.*, 2007; Schmidt, 2016). We therefore used the autoclaved samples as a qualitative control for the null hypothesis that enzymes were responsible for none of the observed substrate hydrolysis, rather than as a quantitative method to distinguish enzymatic substrate hydrolysis from potential abiotic effects. In some sediments, a large fraction of fluorophore can sorb to particles, requiring a correction to observed fluorescence (Coolen *et al.*, 2002; Coolen and Overmann, 2000), but we observed negligible sorption of fluorophore to the White Oak River sediments.

In 2014, enzymes were assayed using a protocol based on the approach of Bell et al (2013), which was designed for soil enzyme assays. In this approach, peptidase substrates were mixed with sediment-buffer slurries in 2-mL wells of a deep-well plate. These plates were periodically centrifuged and 250 µL aliquots of supernatant were transferred into a black 96-well microplate. Fluorescence was read using a BioTek Cytation 3 microplate reader (λ_{ex} = 360 nm, λ_{em} = 440 nm). Results from this method

197 proved considerably noisier than the single-cuvette method used in 2013, so kinetic
198 parameters (V_{max} and K_m) were not calculated for these data. Nevertheless, results were
199 qualitatively similar to those from 2013, and we have reported V_{max} from 2014 as v_0
200 measured at 400 μM substrate concentration, which was saturating. In June 2014, the
201 following substrates were assayed: AAF-AMC, Arg-AMC, Boc-VPR-AMC, D-Phe-
202 AMC, Gly-AMC, Leu-AMC, L-Phe-AMC, Orn-AMC, Z-Phe-Arg-AMC, and Z-Phe-Val-
203 Arg-AMC. In October 2014, L-Phe-AMC, D-Phe-AMC, and Orn-AMC were assayed
204 according to the same protocol in 3-cm core sections at 1.5, 4.5, 7.5, 10.5, 19.5, 22.5,
205 25.5, 28.5, 34.5, 37.5, 40.5, 43.5, 49.5, 52.5, 58.5, and 61.5 cmbsf.

206 GEOCHEMICAL AND MICROBIOLOGICAL MEASUREMENTS

207 Sediment porosity was measured by mass after drying at 80 °C, according to the equation
208

$$\phi = \frac{m_w/\rho_w}{m_w/\rho_w + \frac{m_d - S \times m_w/1000}{\rho_{ds}}}$$

209
210

211 Here, m_w represents mass lost after drying, ρ_w represents the density of pure water, m_d
212 represents the mass of the dry sediment, S represents salinity in g kg^{-1}, and ρ_{ds} represents
213 the density of dry sediment (assumed to be 2.5 g cm^{-3}). Porewater sulfate concentrations
214 were measured using a Dionex Ion Chromatograph (Sunnyvale, CA) in porewater that
215 was separated by centrifugation in 15 ml centrifuge tubes at 5000 × g for 5 minutes,
216 filtered at 0.2 μm, and acidified with 10% HCl. Methane was measured using 3 ml
217 sediment subsamples that were collected from a cutoff syringe, entering through the side

of a core section, immediately after core extrusion. Subsamples were deposited immediately in a 20 ml serum vial containing 1 ml, 0.1 M KOH. These were immediately stoppered and shaken to mix sediment with KOH. Methane was later measured by injecting 500 µl of bottle headspace into a GC-FID (Agilent, Santa Clara, CA) using a headspace equilibrium method (Lapham *et al.*, 2008).

CELL ENUMERATION

Cells were enumerated by direct microscopic counts. One mL of sediment was placed in a 2-mL screw-cap tube with 500 µl of 3% paraformaldehyde in phosphate buffered saline (PBS), in which it was incubated overnight before being centrifuged for 5 minutes at 3000 × *g*. The supernatant was removed and replaced with 500 µl of PBS, vortexed briefly and centrifuged again at 3000 × *g*. The supernatant was subsequently removed and replaced with a 1:1 PBS:ethanol solution. Sediments were then sonicated at 20% power for 40 seconds to disaggregates cells from sediments and diluted 40-fold into PBS prior to filtration onto a 0.2 µm polycarbonate filter (Fisher Scientific, Waltham, MA) and mounted onto a slide. Cells were stained with 4',6-diamidino-2-phenylindole (DAPI) and enumerated by direct counts using a Leica Epifluorescence Microscope.

GEOCHEMICAL MODELING

Organic carbon remineralization rates as a function of depth were estimated by applying a multi-component reaction-transport model to depth distributions of sulfate and methane concentration. The model is based on equations described in Boudreau (1996) and includes only sulfate reduction and methane production due to lack of data regarding oxic and suboxic processes. Thus the model is limited to depths greater than 4.5 cm

where sulfate reduction and methane production are the dominant processes, and bioirrigation and bioturbation may be assumed to be negligible. The organic matter remineralization rate is parameterized using the multi-G model first proposed by Jørgensen (1978); a two-component model was sufficient to accurately simulate the sulfate and methane data. For solutes, the upper boundary conditions were measured values at 4.5 cm while the lower boundary conditions (200 cm) were set to zero-gradient. The flux of reactive organic carbon to 4.5 cm was calculated from the sulfate flux across the 4.5 cm horizon and an estimate of methane burial below the lower boundary (the methane flux at the upper boundary was observed to be zero), with an assumed oxidation state of reactive carbon of -0.7. The model contains four adjustable parameters that are set to capture the major details of measured sulfate and methane data: first-order rate constants for both fractions of the reactive carbon pool; the partitioning factor for both fractions, and the rate constant for methane oxidation.

Results and Discussion

A total of 3739 genes encoding extracellular peptidases were identified among metagenomes from the three depth zones examined, including 685 from SRZ, 1994 from SMTZ, and 1060 from MRZ. Of the genes encoding for peptidases, 0-71% (depending on class of peptidase, algorithm and sediment depth) contained a signal peptide and are likely secreted by the SEC-dependent transport system (Supplementary Table 3). Among the genes with signal peptidases, zinc carboxypeptidases, peptidases of class C25 and genes of the clostripain family are most likely to be secreted. Alternative secretion pathways, which do not rely on signal peptides and therefore would not be identified by

263 the algorithms we used, are also known to exist. These include Sec-independent secretion
264 systems (Bendtsen *et al.*, 2005) and release of cytoplasmic enzymes by cell lysis. The
265 relative importance of these pathways in sediments has not been assessed. At all three
266 depths, peptidases of class C25, belonging to the gingipain family, were the most
267 abundant extracellular peptidases (Fig 1a). Gingipains are endopeptidases (i.e., enzymes
268 that cleave proteins mid-chain rather than from the N- or C-termini) with strong
269 specificity for the residue arginine on the N-terminal side of the scissile bond (Rawlings
270 and Barrett, 1999). Bathyarchaeota, which are abundant in sediments of the White Oak
271 River, use extracellular gingipain (among other peptidases) to degrade detrital protein-
272 like organic matter (Kubo *et al.*, 2012; Lloyd *et al.*, 2013b). Genes annotated as encoding
273 extracellular methionine aminopeptidases and zinc carboxypeptidases were also
274 abundant. The composition of protein families was generally consistent with depth, but
275 genes for clostripain (another endopeptidase with preference for Arg N-terminal to the
276 scissile bond) and S24 peptidases (a regulatory peptidase involved in the SOS stress
277 response) were slightly enriched in the SMTZ.

278 In SRZ, Bacteria accounted for 61% of genes for extracellular peptidases for
279 which a lineage could be assigned, increasing to 69% in MRZ (Fig 1b). Archaeal
280 peptidases decreased from 39% in SRZ to 30% in MRZ, while Eukaryota accounted for
281 <1.5% at all depths. Consistent with this distribution, bacteria make up ca. 40-60% of
282 cells in White Oak River sediments as determined by CARD-FISH counts, with no
283 pronounced depth trend (Lloyd *et al.*, 2013a). Since the majority of the archaeal
284 peptidases in the SRZ were assigned to genomic bins, we were able to accurately classify
285 them. Interestingly, over half of the archaeal SRZ peptidases belong to marine benthic

group D (MBG-D) genomic bins (Fig 1c)(Lazar *et al.*, 2016). Additionally, a large portion of the peptidases in the SRZ belong to newly described Archaea belonging to the Asgard superphylum (Zaremba-Niedzwiedzka *et al.*) including Lokiarchaeota (Spang *et al.*, 2015) and Thorarchaeota (Seitz *et al.*, 2016). Little is known about the ecological roles of these novel Archaea. It has recently been shown that they contain metabolic pathways for the degradation of proteins and acetogenesis (Seitz *et al.*, 2016). Sources of bacterial peptidases varied less with depth than sources of archaeal peptidases, with Proteobacteria, Bacteroidetes, and Firmicutes among the dominant phyla (Fig 1d). 13-20% of extracellular peptidase genes belonged to bacteria but could not be assigned a phylum, and 19-22 phyla contributed extracellular peptidases at each depth. Deltaproteobacteria and Gammaproteobacteria dominated the SRZ community at the White Oak River (Baker *et al.*, 2015), and accordingly the largest portion of the extracellular peptidases also belong to them. These phylogenetic groups decrease with depth in the SMTZ and MRZ, however, Deltaproteobacteria contribute a large portion of extracellular peptidases downcore. Although these groups are commonly thought to rely on sulfur and nitrogen respiration, these genomes were shown to contain metabolic pathways for the degradation and fermentation of organic carbon (Baker *et al.*, 2015). Additionally, several phyla thought to be involved in fermentation of detrital carbon including *Clostridia*, *Bacteroidetes*, *Planctomycetes*, and the candidate phyla radiation (CPR) constitute larger portions of the peptidases in the SMTZ and MRZ.

Bioinformatic tools are a powerful way to investigate the potential of microbial communities to oxidize complex organic molecules, but these tools do not provide information about the expression level of genes or the in situ activities of gene products

and annotation algorithms often fail to identify the precise function of hydrolases, particularly in deeply-branching lineages (e.g., Michalska *et al.*, 2015). Thus, we measured the potential activities of a wide range of extracellular peptidases in the WOR sediments. In 2013 (when the assay protocol used was more sensitive), all six peptidase substrates tested were hydrolyzed faster in untreated sediments than in autoclaved controls (Fig 2, Fig S2). Kinetics of substrate hydrolysis were qualitatively consistent with the Michaelis-Menten rate law,

$$v_0 = (V_{max} + [S])/(K_m + [S]),$$

which is characteristic of purified hydrolases as well as mixtures of isofunctional enzymes in environmental samples (Steen *et al.*, 2015; Sinsabaugh *et al.*, 2014). Together, these lines of evidence show that the observed substrate hydrolysis was due to extracellular peptidases rather than abiotic factors. Combining data from all three sampling dates, unambiguous hydrolysis of eleven different peptidase substrates was observed.

The diverse substrates used in this study were apparently cleaved by a wide variety of peptidases, including aminopeptidases (peptidases that cleave an N-terminal amino acid from a protein) and endopeptidases (peptidases that cleave internal peptide bonds). Peptide bonds adjacent to a diverse set of amino acid residues were cleaved, including glycine (the smallest amino acid), phenylalanine (among the largest amino acids), arginine (positively charged at porewater pH) and leucine (uncharged, hydrophobic). Individual extracellular peptidases can often accept a fairly broad range of

substrates, and sometimes a substrate may primarily be hydrolyzed by an enzyme that exhibits maximal activity towards a different substrate. For instance, in pelagic samples from Bogue Sound, an estuary in North Carolina, the substrate Leu-AMC, which is putatively a substrate for leucine aminopeptidase, was hydrolyzed more by arginine aminopeptidase than by leucine aminopeptidase (Steen *et al.*, 2015). Nevertheless, the large diversity of substrates that were hydrolyzed in this study suggests a diverse set of extracellular peptidases present in sediments, as has previously been observed in pelagic samples (Obayashi and Suzuki, 2008, 2005; Steen and Arnosti, 2013).

Bulk potential enzyme activities (V_{max} values) decreased with increasing depth (Fig 3a). However, no trend was evident in V_{max} values expressed per cell (Fig 3b), and V_{max} expressed relative to bulk organic carbon oxidation rate increased downcore by more than two orders of magnitude (Figs 3c-d). V_{max} per cell was approximately 100-200 amol cell^{-1} hr^{-1} throughout the core, comparable to previous measurements made in a surface sediments (2-100 amol cell^{-1} hr^{-1}) and surface seawater (mostly less than 100 amol cell^{-1} hr^{-1}, but with some measurements up to 10 nmol cell^{-1} hr^{-1}) (Vetter and Deming, 1994). Modeled organic carbon oxidation due to sulfate reduction and methane production decreased from 9315 µmol C (g wet sediment)$^{-1}$ hr^{-1} at 4.5 cmbsf (the top of the model domain) to 18 µmol C (g wet sediment^{-1}) hr^{-1} at 82.5 cmbsf, a decrease of a factor of 518. The sum of V_{max} of all peptidases measured in 2013 decreased from 94.7 µmol g sed^{-1} hr^{-1} at 1.5 cmbsf to 12.8 µmol g sed^{-1} hr^{-1} at 82.5 cmbsf depth, a decrease of a factor of 7.4. The value of the V_{max}:OC oxidation rate ratio is sensitive to the precise set of enzyme included in the sum (it is likely that some peptidases exist in the sediment that were not measured, and that some promiscuous enzymes are double-counted because they

355 hydrolyze more than one substrate), but the trend is clear: as sediment depth increased,
356 the potential activity of extracellular peptidases increased faster than the actual rate of
357 organic carbon oxidation. V_{max} is a proxy for the concentration of enzymes in an
358 environment, so the observed increase in V_{max} relative to OC oxidation rate suggests that
359 subsurface microbial communities produced similar quantities of enzyme per cell as
360 surface communities, but that those enzymes returned less bioavailable organic matter,
361 presumably due to lower substrate concentrations.

362 In the sense of bulk activities, therefore, subsurface heterotrophic communities in
363 WOR seem to be similar their surface counterparts in terms of reliance on extracellular
364 enzymes to access organic matter, although metabolisms are slower in the subsurface.
365 However, there are indications from enzyme kinetics and activities of specific enzymes
366 that subsurface communities are specialized for their environment. Peptidase K_m values
367 decreased with increasing depth (Fig 4, Fig S3, ANCOVA, $F(5, 22)=4.44$, $p < 0.05$).
368 When substrate concentrations are considerably less than K_m, as they likely are in
369 subsurface sediments, *in situ* substrate hydrolysis rates are controlled more by K_m than by
370 V_{max} (Steen and Ziervogel, 2012; Cornish-Bowden, 2012), so decreasing K_m values may
371 be an adaptive response to low bioavailable substrate concentrations in subsurface
372 sediments (Sinsabaugh *et al.*, 2014).

373 The trends in K_m warrant some discussion of how K_m values are measured and
374 interpreted. As with all environmental enzyme assays, our measurements relied on
375 measuring the rate of reaction of an artificial substrate that was added to the sample. The
376 sample also contained some quantity of natural substrate (i.e., proteins or peptides). This
377 naturally-present substrate can be viewed as a competitive inhibitor of the added artificial

substrate (Cornish-Bowden, 2012). As a consequence, the K_m we measure ($K_{m,app}$) is actually the sum of the true enzyme K_m plus the concentration of *in situ* enzyme substrate ($[S_{is}]$); $K_{m,app} = K_m + [S_{is}]$. It is therefore possible that the observed decrease in $K_{m,app}$ actually reflects a change in the concentration of natural peptidase substrates with depth, rather than a change in substrate affinity of peptidases. $[S_{is}]$ is extremely difficult to measure (or even to define precisely) because it reflects the sum of the concentrations of all of the individual molecules which can act as substrate for a given peptidase, weighted by the degree to which the peptidase is capable of accessing each substrate. $[S_{is}]$ almost certainly decreased downcore, since a decrease in the concentration of enzymatically-hydrolyzable, protein-like organic matter is a diagnostic feature of aged organic matter (Amon *et al.*, 2001; Dauwe *et al.*, 1999). However, it is very unlikely that $[S_{is}]$ could have decreased enough to cause more than a negligible fraction of the observed decreases in K_m, which were ranged from 110 μM (GGR-AMC) to 990 μM (AAF-AMC). Sediments of Aarhus Bay, which are similar to those of the White Oak River in terms of organic matter content and grain size, are characterized by porewater dissolved combined amino acid concentrations in the range of 50-150 μM L^{-1} (Pedersen *et al.*, 2001). Only a fraction of that dissolved protein-like material can act as substrate for any given peptidase. 10-40% of total combined amino acids in sediments were accessible to a peptidase which was specifically selected because of its ability to hydrolyze diverse proteins (Dauwe *et al.*, 1999), and a smaller fraction may be available to the individual peptidases measured in this study. Furthermore, K_m values were measured in a 9:1 buffer:sample slurry, so $[S_{is}]$ in the slurry would be one-tenth of *in situ* $[S_{is}]$. By multiplying assumed porewater substrate concentrations (from Aarhus Bay) by the fraction that is enzymatically

401 hydrolysable and dividing by 10 to account for dilution in the slurry, we estimate that
402 changes in [S_{is}] could account for, at most, a 0.5-6 μM decrease in $K_{m,app}$. The remainder
403 of the 110-990 μM decrease must be due to changes in the true substrate affinity K_m,
404 indicating that subsurface enzymes hydrolyze low concentrations of protein considerably
405 more efficiently than surface enzymes.

406 The suite of specific peptidases that are active in deeper sediments also seems to
407 reflect adaptation to more degraded organic matter. In order to assess the degree to which
408 sedimentary extracellular peptidases target more recalcitrant organic matter, rather than
409 the extremely small pool of relatively labile organic matter, in 2014 we compared
410 potential activities of D-phenylalanyl aminopeptidase (D-PheAP) and ornithine
411 aminopeptidase (OrnAP) to those of L-phenylalanyl aminopeptidase (L-PheAP). D-
412 phenylalanine and ornithine are both markers for degraded organic matter. Most amino
413 acids are biosynthesized as L-stereoisomers. D-stereoisomers in sedimentary organic
414 matter can be produced via abiotic racemization of biomass (Bada and Schroeder, 1975;
415 Steen *et al.*, 2013) or by bacterial reprocessing of phytoplankton-derived OM (Pedersen
416 *et al.*, 2001; Kaiser and Benner, 2008; Lomstein *et al.*, 2006). Ornithine is non-
417 proteinogenic amino acid, which does not exist in high concentration in fresh biomass,
418 but which can be produced in sediments via deamination of arginine and therefore
419 indicates OM degradation (Hare, 1968; Lee and Cronin, 1984). L-phenylalanine is among
420 the most recalcitrant amino acids (Dauwe and Middelburg, 1998) but is more labile than
421 D-phenylalanine or ornithine, so we take L-PheAP activity as a marker of the
422 community's ability to access relatively fresh OM.

D-PheAP:L-PheAP and OrnAP:L-PheAP ratios increased significantly with depth (Fig 5, D-PheAP:L-Phe-AP: $p<0.01$, $r^2=0.35$, n=16; OrnAP:L-PheAP: $p < 0.05$, $r^2=0.26$, n=16), indicating that subsurface communities expressed peptidases that release amino acids from relatively recalcitrant organic matter. These results do not indicate the actual flux of organic matter to communities: V_{max} reflects a potential rate at saturating substrate concentrations, not an *in situ* rate. Nevertheless, these results suggest that deeper heterotrophic communities seek to access the larger pool of more recalcitrant organic matter rather than the smaller pool of more labile organic matter.

In summary, genetic analysis and enzyme assays reveal that a diverse set of extracellular peptidases are present throughout the top 83 cm of White Oak River estuary sediments, and that these enzymes are produced by a wide range of Bacteria and Archaea. Surface and subsurface communities express similar quantities of extracellular peptidase per cell, but subsurface peptidases catalyze reactions much more slowly, likely because concentrations of enzyme-labile substrates are much lower in the subsurface. This implies selective pressure on subsurface communities to produce extracellular enzymes that function more effectively in the presence of low concentrations of more-degraded organic matter. Accordingly, subsurface enzymes showed higher affinity (lower K_m) than surface enzymes, and the mix of subsurface enzymes shifted towards enzymes such as D-phenylalanine aminopeptidase and ornithine aminopeptidase. These shifts are consistent with community-level adaptation to heterotrophic communities to subsurface organic matter, although we lack data as to whether that adaptation is caused by evolution of surface communities as sediment is buried or selective survival of taxa that are more capable of accessing degraded organic matter. Further analysis of the mechanisms by

446 which subsurface heterotrophs access sedimentary organic matter may yield continued

447 insights into how heterotrophic microorganisms live in low-energy environments such as

448 subsurface sediments.

449

450

Acknowledgements

We thank Michael Piehler for access to his laboratory facilities at the University of North Carolina Institute of Marine Sciences, the captain of the R/V Capricorn for sampling assistance, and Terry Hazen for use of lab equipment at the University of Tennessee. We thank Oliver Jeffers for reminding ADS that science is cool. Funding for KHM was provided by NSF grant DBI-1156644 to Steven W. Wilhelm. Funding for ADS was provided by NSF grant OCE-1431598 and a C-DEBI subaward. This work is C-DEBI Contribution number <<to be determined.>>

Conflict of interest

The authors declare no competing financial interests in relation to the work described.

464 # References

465 Allison SD. (2005). Cheaters, diffusion and nutrients constrain decomposition by
466 microbial enzymes in spatially structured environments. *Ecol Lett* **8**: 626–635.
467 Amon RMW, Fitznar H-P, Benner R. (2001). Linkages among the bioreactivity, chemical
468 composition, and diagenetic state of marine dissolved organic matter. *Limnol*
469 *Oceanogr* **46**: 287–297.
470 Bada JL, Schroeder RA. (1975). Amino acid racemization reactions and their
471 geochemical implications. *Naturwissenschaften* **62**: 71–79.
472 Bagos PG, Tsirigos KD, Plessas SK, Liakopoulos TD, Hamodrakas SJ. (2009).
473 Prediction of signal peptides in archaea. *Protein Eng Des Sel* **22**: 27–35.
474 Baker BJ, Lazar CS, Teske AP, Dick GJ. (2015). Genomic resolution of linkages in
475 carbon, nitrogen, and sulfur cycling among widespread estuary sediment bacteria.
476 *Microbiome* **3**: 14.
477 Baker BJ, Saw JH, Lind AE, Lazar CS, Hinrichs K-U, Teske AP, *et al.* (2016). Genomic
478 inference of the metabolism of cosmopolitan subsurface Archaea, Hadesarchaea. *Nat*
479 *Microbiol* **1**: 16002.
480 Bell CW, Fricks BE, Rocca JD, Steinweg JM, McMahon SK, Wallenstein MD. (2013).
481 High-throughput fluorometric measurement of potential soil extracellular enzyme
482 activities. *J Vis Exp* e50961.
483 Bendtsen JD, Kiemer L, Fausbøll A, Brunak S. (2005). Non-classical protein secretion in
484 bacteria. *BMC Microbiol* **5**: 58.
485 Benner R, Amon RMW. (2015). The size-reactivity continuum of major bioelements in
486 the ocean. *Ann Rev Mar Sci* **7**: 185–205.

487 Benz R, Bauer K. (1988). Permeation of hydrophilic molecules through the outer
488 membrane of gram-negative bacteria. Review on bacterial porins. *Eur J Biochem* **176**:
489 1–19.
490 Biddle JF, Lipp JS, Lever MA, Lloyd KG, Sørensen KB, Anderson R, *et al.* (2006).
491 Heterotrophic Archaea dominate sedimentary subsurface ecosystems off Peru. *Proc*
492 *Natl Acad Sci U S A* **103**: 3846–51.
493 Blair CC, D'Hondt S, Spivack AJ, Kingsley RH. (2007). Radiolytic hydrogen and
494 microbial respiration in subsurface sediments. *Astrobiology* **7**: 951–70.
495 Boudreau BP. (1996). A method-of-lines code for carbon and nutrient diagenesis in
496 aquatic sediments. *Comput Geosci* **22**: 479–496.
497 Burdige DJ. (2007). Preservation of organic matter in marine sediments: controls,
498 mechanisms, and an imbalance in sediment organic carbon budgets? *Chem Rev* **107**:
499 467–85.
500 Carter DO, Yellowlees D, Tibbett M. (2007). Autoclaving kills soil microbes yet soil
501 enzymes remain active. *Pedobiologia (Jena)* **51**: 295–299.
502 Coolen MJL, Cypionka H, Sass AM, Sass H, Overmann J. (2002). Ongoing modification
503 of Mediterranean Pleistocene sapropels mediated by prokaryotes. *Science* **296**: 2407–
504 10.
505 Coolen MJL, Overmann J. (2000). Functional Exoenzymes as Indicators of Metabolically
506 Active Bacteria in 124,000-Year-Old Sapropel Layers of the Eastern Mediterranean
507 Sea. *Appl Environ Microbiol* **66**: 2589–2598.
508 Cornish-Bowden A. (2012). Fundamentals of enzyme kinetics. Fourth Edition. Wiley-
509 VCH Verlag & Co. KGaA: Weinheim.

510 Dauwe B, Middelburg JJ. (1998). Amino acids and hexosamines as indicators of organic
511 matter degradation state in North Sea sediments. *Limnol Oceanogr* **43**: 782–798.
512 Dauwe B, Middelburg JJ, Van Rijswijk P, Sinke J, Herman PMJ, Heip CHR. (1999).
513 Enzymatically hydrolyzable amino acids in North Sea sediments and their possible
514 implication for sediment nutritional values. *J Mar Res* **57**: 109–134.
515 Gruebel KA, Martens CS. (1984). Radon-222 tracing of sediment-water chemical
516 transport in an estuarine sediment. *Limnol Oceanogr* **29**: 587–597.
517 Hare PE. (1968). Geochemistry of Proteins, Peptides, and Amino Acids. In: Eglinton G,
518 Murphy MTJ (eds). *Organic Geochemistry: Methods and Results*. Springer-Verlag:
519 Berlin, Heidelberg, pp 438–462.
520 Hiller K, Grote A, Scheer M, Münch R, Jahn D. (2004). PrediSi: Prediction of signal
521 peptides and their cleavage positions. *Nucleic Acids Res* **32**. e-pub ahead of print, doi:
522 10.1093/nar/gkh378.
523 Jacobson Meyers ME, Sylvan JB, Edwards KJ. (2014). Extracellular enzyme activity and
524 microbial diversity measured on seafloor exposed basalts from Loihi seamount
525 indicate the importance of basalts to global biogeochemical cycling. *Appl Environ*
526 *Microbiol* **80**: 4854–64.
527 Jørgensen BB. (1978). A comparison of methods for the quantification of bacterial sulfate
528 reduction in coastal marine sediments: II. Calculation from mathematical models.
529 *Geomicrobiol J* **1**: 29–47.
530 Jørgensen BB, Marshall IPG. (2016). Slow Microbial Life in the Seabed. *Ann Rev Mar*
531 *Sci* **8**: 311–32.
532 Kaiser K, Benner R. (2008). Major bacterial contribution to the ocean reservoir of detrital

organic carbon and nitrogen. *Limnol Oceanogr* **53**: 99–112.

Kallmeyer J, Pockalny R, Adhikari RR, Smith DC, D'Hondt S. (2012). Global distribution of microbial abundance and biomass in subseafloor sediment. *Proc Natl Acad Sci U S A* **109**: 16213–6.

Kelley CA, Martens CS, Chanton JP. (1990). Variations in sedimentary carbon remineralization rates in the White Oak River estuary, North Carolina. *Limnol Oceanogr* **35**: 372–383.

Kubo K, Lloyd KG, F Biddle J, Amann R, Teske A, Knittel K. (2012). Archaea of the Miscellaneous Crenarchaeotal Group are abundant, diverse and widespread in marine sediments. *ISME J* **6**: 1949–65.

Lapham LL, Chanton JP, Martens CS, Sleeper K, Woolsey JR. (2008). Microbial activity in surficial sediments overlying acoustic wipeout zones at a Gulf of Mexico cold seep. *Geochemistry, Geophys Geosystems* **9**: Q06001.

Lazar CS, Baker BJ, Seitz K, Hyde AS, Dick GJ, Hinrichs K-U, *et al.* (2016). Genomic evidence for distinct carbon substrate preferences and ecological niches of Bathyarchaeota in estuarine sediments. *Environ Microbiol* **18**: 1200–11.

Lee C, Cronin C. (1984). Particulate amino acids in the sea: Effects of primary productivity and biological decomposition. *J Mar Res* **42**: 1075–1097.

Lloyd KG, Alperin MJ, Teske A. (2011). Environmental evidence for net methane production and oxidation in putative ANaerobic MEthanotrophic (ANME) archaea. *Environ Microbiol* **13**: 2548–2564.

Lloyd KG, May MK, Kevorkian RT, Steen AD. (2013a). Meta-analysis of quantification methods shows that archaea and bacteria have similar abundances in the subseafloor.

556 *Appl Environ Microbiol* **79**: 7790–9.

557 Lloyd KG, Schreiber L, Petersen DG, Kjeldsen KU, Lever M a, Steen AD, *et al.* (2013b).
558 Predominant archaea in marine sediments degrade detrital proteins. *Nature* **496**: 215–
559 8.

560 Lomstein B, Jorgensen B, Schubert C, Niggemann J. (2006). Amino acid biogeo- and
561 stereochemistry in coastal Chilean sediments. *Geochim Cosmochim Acta* **70**: 2970–
562 2989.

563 Martens CS, Goldhaber MB. (1978). Early diagenesis in transitional sedimentary
564 environments of the White Oak River Estuary, North Carolina. *Limnol Oceanogr* **23**:
565 428–441.

566 Meng J, Xu J, Qin D, He Y, Xiao X, Wang F. (2014). Genetic and functional properties
567 of uncultivated MCG archaea assessed by metagenome and gene expression analyses.
568 *ISME J* **8**: 650–9.

569 Michalska K, Steen AD, Chhor G, Endres M, Webber AT, Bird J, *et al.* (2015). New
570 aminopeptidase from 'microbial dark matter' archaeon. *FASEB J* **29**: 4071–4079.

571 Obayashi Y, Suzuki S. (2008). Occurrence of exo- and endopeptidases in dissolved and
572 particulate fractions of coastal seawater. *Aquat Microb Ecol* **50**: 231–237.

573 Obayashi Y, Suzuki S. (2005). Proteolytic enzymes in coastal surface seawater:
574 Significant activity of endopeptidases and exopeptidases. *Limnol Oceanogr* **50**: 722–
575 726.

576 Pedersen A-GU, Thomsen TR, Lomstein BA, Jørgensen NOG. (2001). Bacterial
577 influence on amino acid enantiomerization in a coastal marine sediment. *Limnol*
578 *Oceanogr* **46**: 1358–1369.

579 Petersen TN, Brunak S, von Heijne G, Nielsen H. (2011). SignalP 4.0: discriminating
580 signal peptides from transmembrane regions. *Nat Methods* **8**: 785–6.
581 Rawlings ND, Barrett AJ. (1999). MEROPS: The peptidase database. *Nucleic Acids Res*
582 **27**: 325–331.
583 Schimel JP, Weintraub MN. (2003). The implications of exoenzyme activity on microbial
584 carbon and nitrogen limitation in soil: a theoretical model. *Soil Biol Biochem* **35**:
585 549–563.
586 Schmidt J. (2016). Microbial Extracellular Enzymes in Marine Sediments: Methods
587 Development and Potential Activities in the Baltic Sea Deep Biosphere. University of
588 Tennessee - Knoxville.
589 Seitz KW, Lazar CS, Hinrichs K-U, Teske AP, Baker BJ. (2016). Genomic
590 reconstruction of a novel, deeply branched sediment archaeal phylum with pathways
591 for acetogenesis and sulfur reduction. *ISME J* **10**: 1696–1705.
592 Sinsabaugh RL, Belnap J, Findlay SG, Shah JJF, Hill BH, Kuehn KA, *et al.* (2014).
593 Extracellular enzyme kinetics scale with resource availability. *Biogeochemistry* **121**:
594 287–304.
595 Spang A, Saw JH, Jørgensen SL, Zaremba-Niedzwiedzka K, Martijn J, Lind AE, *et al.*
596 (2015). Complex archaea that bridge the gap between prokaryotes and eukaryotes.
597 *Nature* **521**: 173–179.
598 Steen AD, Arnosti C. (2013). Extracellular peptidase and carbohydrate hydrolase
599 activities in an Arctic fjord (Smeerenburgfjord, Svalbard. *Aquat Microb Ecol* **69**: 93–
600 99.
601 Steen AD, Arnosti C. (2011). Long lifetimes of β-glucosidase, leucine aminopeptidase,

602 and phosphatase in Arctic seawater. *Mar Chem* **123**: 127–132.

603 Steen AD, Jørgensen BB, Lomstein BA. (2013). Abiotic Racemization Kinetics of
604 Amino Acids in Marine Sediments. *PLoS One* **8**. e-pub ahead of print, doi:
605 10.1371/journal.pone.0071648.

606 Steen AD, Vazin JP, Hagen SM, Mulligan KH, Wilhelm SW. (2015). Substrate
607 specificity of aquatic extracellular peptidases assessed by competitive inhibition
608 assays using synthetic substrates. *Aquat Microb Ecol* **75**: 271–281.

609 Steen AD, Ziervogel K. (2012). Comment on the review by German et
610 al.(2011)‘Optimization of hydrolytic and oxidative enzyme methods for ecosystem
611 studies’[Soil Biology & Biochemistry 43: 1387--1397]. *Soil Biol Biochem* **48**: 196–
612 197.

613 Stursova M, Sinsabaugh RL. (2008). Stabilization of oxidative enzymes in desert soil
614 may limit organic matter accumulation. *Soil Biol Biochem* **40**: 550–553.

615 Vetter YA, Deming JW. (1994). Extracellular enzyme activity in the Arctic Northeast
616 Water polynya. *Mar Ecol Prog Ser* **114**: 23–34.

617 Vetter Y, Deming J, Jumars P, Krieger-Brockett B. (1998). A Predictive Model of
618 Bacterial Foraging by Means of Freely Released Extracellular Enzymes. *Microb Ecol*
619 **36**: 75–92.

620 Yu NY, Wagner JR, Laird MR, Melli G, Rey S, Lo R, *et al.* (2010). PSORTb 3.0:
621 improved protein subcellular localization prediction with refined localization
622 subcategories and predictive capabilities for all prokaryotes. *Bioinformatics* **26**:
623 1608–1615.

624 Zaremba-Niedzwiedzka K, Caceres E, Saw J, Backstrom D, Juzokaite L, Vancaester E, *et*

al. Metagenomic exploration of Asgard arcahea illuminates the origin of eukaryotic cellular complexity.

Figure Legends

Fig 1: (A) Frequency of genes for various classes of extracellular peptidases, relative to all genes for extracellular peptidases; (b) sources of extracellular peptidases by domain and depth; and sources of (c) Archaeal and (d) Bacterial peptidases by phylum and depth.

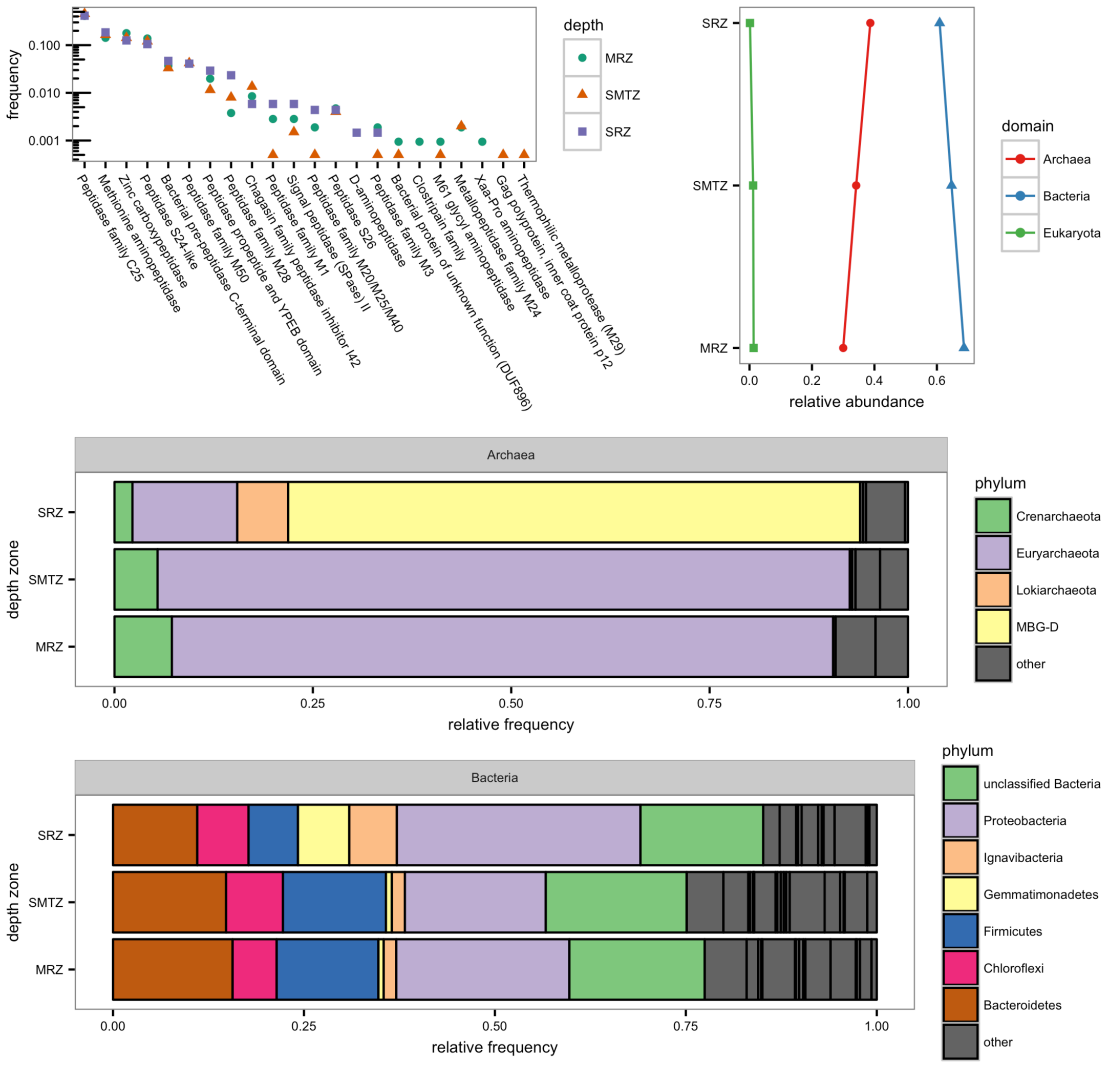

637 Fig 2: Peptidase saturation curves, showing Michealis-Menten kinetics consistent with

638 enzymatic rather than abiotic substrate hydrolysis. Open triangles indicate autoclaved

639 controls.

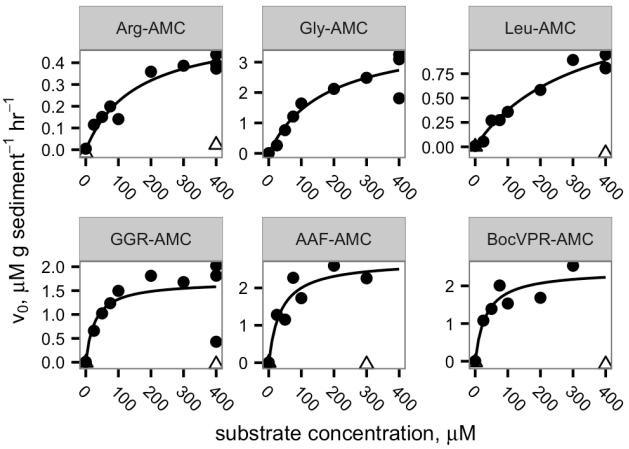

640

641

642

643 Fig 3: Peptidase activities compared to microbial abundance and activity. Panel A:
644 summed V_{max} of the six peptidases measured in 2013, expressed relative to the value at
645 1.5 cm. Error bars represent standard error of the estimate of the rate of fluorophore
646 production. B: Summed V_{max} relative to cell abundance. Error bars represent error
647 propagated from error of Vmax and standard deviation of cell counts. C: Modeled
648 organic carbon oxidation rate. D: Summed V_{max} relative to organic carbon oxidation rate.
649 Error bars represent standard error of the estimate of the rate of fluorophore production.

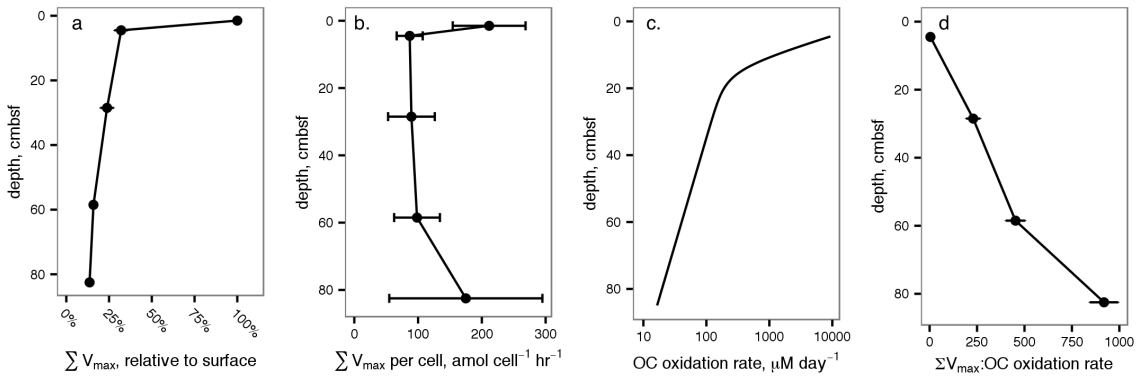

650

651

652 Fig 4: Estimated K_m values as a function of sediment depth. Colored lines indicate linear
653 regressions for individual substrates, while the black line and shaded area represent a
654 regression for all substrates taken together.

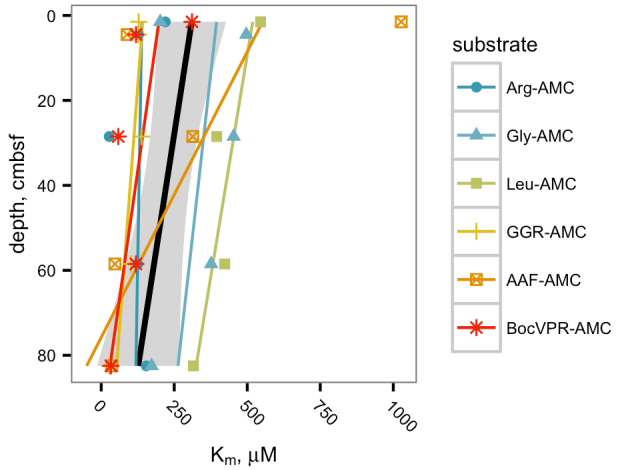

655
656

657 Fig 5: Left panel: Ratio of D-phenylalanyl aminopeptidase V_{max} to L-phenylalanyl

658 aminopeptidase V_{max} versus depth. Right panel: Ratio of ornithyl aminopeptidase V_{max} to

659 L-phenylalanyl aminopeptidase V_{max}. The shaded band indicates the 95% confidence

660 interval of the fitted values.

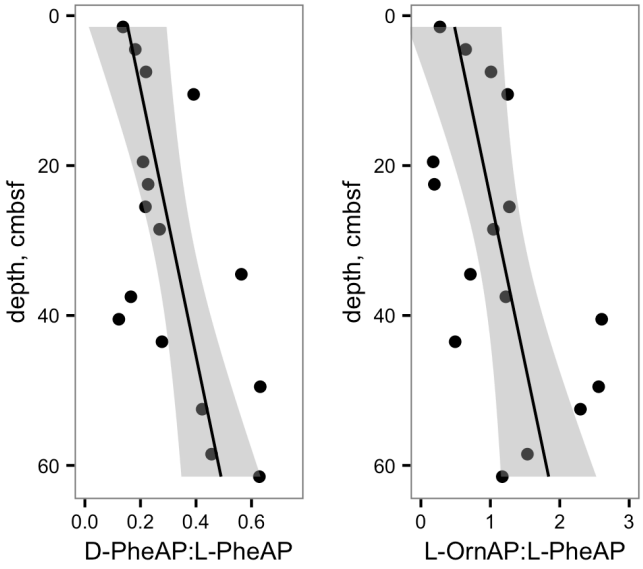

661